Juan R. Mosig

# Roger F. Harrington and the Method of Moments

## Part 1: Electrostatics.

xxxxx

The method of moments (MOM), as introduced by R. F. Harrington more than 50 years ago, is reviewed in the context of the classic potential integral equation (PIE) formulations applied to both electrostatic (part 1) and electrodynamic, or full-wave, problems (part 2). A systematic treatment is presented based on the concept of "discrete Green's functions" ("GFs"). For the sake of simplicity and clarity, the developments are restricted to geometries composed of 2D metallic plates embedded in a homogeneous medium. Within this framework, original analytical developments are presented. They simplify the formulations and enable the implementation of point matching (PM) and Galerkin strategies without any need for a numerical evaluation of the involved multidimensional integrals. Simple MATLAB codes are provided, allowing the reader not only to reproduce but also to go beyond the pioneering results of Harrington, to whom this article pays an undisguised homage.

## INTRODUCTION

More than 50 years ago, in 1968, a book was published that would change forever the numerical approaches used in computational electromagnetics and, more specifically, in antenna and microwave engineering. Its title was *Field Computation by Moment Methods* [1], and its author, Roger F. Harrington, was then a young professor at Syracuse University, Syracuse, NY, USA. As Prof. Harrington himself explained in a very illuminating paper [2] about the history of the genesis of his book, the name "method of moments" (MOM) was selected because it was the name used by the Russian mathematicians Kantorovich and Akilov [3] for a similar method in the realm of functional analysis.

Since its publication, this book has become one of the most cited in our domain (at the moment of writing, Google Scholar mentions almost 13,000 citations), and the number of research papers using the MOM is overwhelming. A good compilation of early MOM papers can be found in the book *Computational Electromagnetics*, subtitled *Frequency Domain Method of Moments* [4]. In the wake of Harrington's book, several books

have been published that generalize the MOM and apply it to highly diverse problems (see, for instance, [5], recently enlarged and reissued). However, this author firmly believes that *Field Computation by Moment Methods* remains the best possible introduction to the method.

In 1968, Prof. Harrington was already a well-known figure in our community, after having published in 1961 another landmark book, *Time-Harmonic Electromagnetic Fields* [6]. Despite this fact, his MOM was not immediately accepted by the specialists. A well-known story, related by Don Wilton [7], tells us that a 1967 *Proceedings of the IEEE* paper [8], anticipating *Field Computation by Moment Methods* and containing a summary of it, had been previously rejected by *IEEE Transactions on Antennas and Propagation*. Reviewers had argued against the possibility of representing continuous quantities, such as electric currents, using discontinuous quantities and against the possibility of inverting a $100 \times 100$ matrix in a computer "because the magnetic tape unit would wear out going back and forth." Times have changed.

In a retrospective paper [9], Jim Rautio, a former student of Harrington, tells us how the 100-unknowns barrier was broken in 1982 by using one of the first IBM PCs rated at 4.77 MHz (!) (solving the linear system took 1 h …) and how 20 years later, he was customarily doing in about 2 h direct matrix solutions of linear systems with 100,000 unknowns, using another IBM PC rated at 2.4 GHz.

Clearly, the amazing increase in computer speed and memory in the last 40 years is one reason for the popularity of the MOM. But we must not neglect the outstanding abilities of Prof. Harrington as a scientific writer in the engineering realm. In his two books [1], [6], the mathematical language is as simple as possible while remaining rigorous. The treatment is always guided by physical interpretation of the subject, and approximations are not ignored if they result in a reasonable tradeoff between the complexity of analytical developments and the accuracy of the results. It is no surprise that these books are electrical engineering bestsellers.

The MOM is a general strategy for solving any linear operator equation and allows us to numerically solve any linear electromagnetic boundary value problem arising from Maxwell's equations [7]. Here, we want to pay homage to Harrington's work and to highlight his achievements by reviewing the MOM formulation for potential-based integral equations. We then revisit some of the simple canonical geometries he studied, using a generalized strategy. This article is in two parts dealing, respectively, with electrostatic and electrodynamic (time-harmonic full-wave) situations.

## THE POTENTIAL INTEGRAL EQUATION FOR METALLIC BODIES

Consider an ideal metallic body [perfect electric conductor (PEC)] illuminated by a known excitation electric field, which can be also expressed as an excitation potential, with the classical relationship $\mathbf{E_{exc}} = -\nabla V_{exc}$.

As a result of this excitation (Figure 1), an unknown surface charge density $\rho_s$ appears on the surface of the body. This charge produces in turn an "induced" electric field/potential

(in electrodynamics, the adjective "induced" is replaced by "scattered"). Basic electrostatic theory tells us that the induced potential at an observation point $\mathbf{r}$ can be expressed as

$$4\pi\varepsilon_0 V_{ind}(\mathbf{r}) = \int_S ds' \, \rho_s(\mathbf{r}')G(\mathbf{r}\,|\,\mathbf{r}') = G \otimes \rho_s. \tag{1}$$

Here, $G(\mathbf{r}\,|\,\mathbf{r}')$ is the pertinent GF, and the convolution notation $\otimes$ has been introduced (in free space, $G(\mathbf{r}\,|\,\mathbf{r}') = 1/(|\mathbf{r} - \mathbf{r}'|)$).

The physics of the problem requires that the induced potential "compensates" the excitation potential, producing a total potential $U$, not necessarily known but constant on the body's surface. This condition allows us to set up a potential integral equation (PIE) for the unknown surface charge density $\rho_s$, which can be written in compact notation as

$$G \otimes \rho_s = 4\pi\varepsilon_0(U - V_{exc}). \tag{2a}$$

The total charge on the body's surface is then given by

$$Q = \int_S ds\rho_s. \tag{2b}$$

In general, either the body has a known potential $U$ (being connected to a battery or grounded) or it has a known total charge $Q$ (an isolated body). In the first situation, the total charge is unknown but can be computed a posteriori using (2b). In the second situation, (2b) provides a supplementary equation allowing us to deal with the additional unknown $U$. Obviously, in the absence of an external excitation ($V_{exc} = 0$), the set of equations (2) can have a nonzero solution for $\rho_s$ only if either $U$ or $Q$ has nonzero values. In the next section, we set up some possible solutions of this PIE using the MOM.

## MOM SOLUTION: SUBSECTIONAL BASIS FUNCTIONS AND DISCRETE GFs

This section deals with some classical developments, fully covered in Harrington's book [1, Secs. 1.3–1.5 and 2.1–2.2]. Here, for the sake of completeness, we briefly revisit the formulation, using a slightly different point of view. The MOM transforms
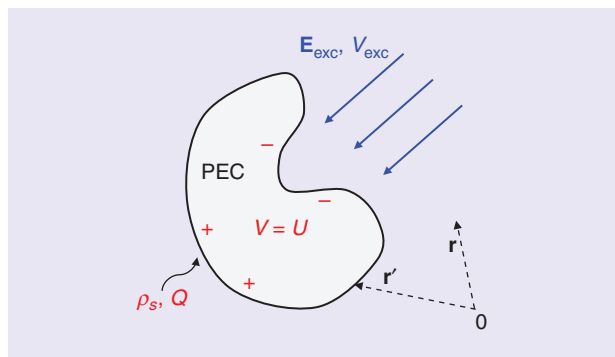


**FIGURE 1.** An excitation electric field $\mathbf{E_{exc}}$ creates a surface charge density $\rho_s$ on a PEC body. The body may have a total nonzero charge $Q$. The electrostatic potential of the body $U$ can be known and imposed by external circumstances (a battery-connected or grounded body) or unknown and to be determined (an isolated body). But in all cases, it remains constant inside the body and on its surface.

the PIE (2) into a linear algebraic system by expanding the unknown charge density into a set of $N$ basis functions $b_j$ as

$$\rho_s = \sum_{j=1}^{N} \alpha_j b_j \tag{3}$$

where $\alpha_j$ are constant expansion coefficients to be determined. Then, the integral equation is projected into a set of test functions $t_i$ with the help of a predefined inner product [1, Sec. 1.2], denoted by $\langle\ \rangle$ and defined here as

$$\langle t_i, f \rangle = \int_{S_i} ds\, t_i(\mathbf{r}) f(\mathbf{r}). \tag{4}$$

The resulting matrix equation can be written as

$$[c_{ij}][\alpha_j] = [e_i]. \tag{5a}$$

The most commonly used basis and test functions are "subsectional" functions, which exist only over subsections ("cells") $S_i$ of the integration domain $S$ [1, Sec. 1.5]. In this article, we use only these functions. With these assumptions, the MOM matrix elements are given by

$$c_{ij} = \langle t_i, G \otimes b_j \rangle = \int_{S_i} ds\, t_i(\mathbf{r}) \int_{S_j} G(\mathbf{r}\,|\,\mathbf{r}') b_j(\mathbf{r}') \tag{5b}$$

and the excitation vector elements by

$$e_i = 4\pi\varepsilon_0 \langle t_i, U - V_{\mathrm{exc}}(\mathbf{r}) \rangle = 4\pi\varepsilon_0 \int_{S_i} ds\, t_i(\mathbf{r})[U - V_{\mathrm{exc}}(\mathbf{r})]. \tag{5c}$$

Quite frequently, we select the same functions for the basis and test, $t_i = b_i$. This is the Galerkin method, endowed with interesting variational properties [1, Sec. 1.8].

In electrostatic problems dealing with surfaces, the simplest possible subsectional basis, used by Harrington, is the piecewise constant basis, mathematically defined as a 2D pulse function $\Pi$ existing over a subsection (cell) of the problem. The pulse amplitude is selected to have either a unit surface charge density or a unit total cell charge. For reasons that become evident soon, we favor this second choice, which results in the definition

$$b_j(\mathbf{r}') = \frac{1}{S_j}\Pi(S_j); \quad \Pi(S_j) = \begin{cases} 1 & \text{if } \mathbf{r}' \in S_j \\ 0 & \text{elsewhere} \end{cases}. \tag{6}$$

We now specialize the Galerkin implementation (5) to these basis functions.

The writing of the final expressions is greatly simplified by the introduction of the so-called discrete GFs and averaged discrete GFs. While a GF always has a point source, the discrete GF, $\Gamma_{ij}$, is obtained when a full basis function is used as the source, and it can be mathematically expressed as

$$\Gamma_{ij} = \Gamma(\mathbf{r}_i, S_j) = \frac{1}{S_j}\int_{S_j} ds'\, G(\mathbf{r}_i\,|\,\mathbf{r}') \tag{7a}$$

where $\mathbf{r}_i$ denotes the center of the test cell $S_i$.

In a subsequent step, we consider the mean value of a discrete GF when the observer point spans a test cell $S_i$. This is the averaged discrete GF, $\Psi_{ij}$, given by

$$\Psi_{ij} = \Psi(S_i, S_j) = \frac{1}{S_i}\int_{S_i} ds\, \Gamma(\mathbf{r}, S_j)$$
$$= \frac{1}{S_i S_j}\int_{S_i} ds \int_{S_j} ds'\, G(\mathbf{r}\,|\,\mathbf{r}'). \tag{7b}$$

In other words, the discrete GF is a "basis-integrated GF," given by the mean value of the corresponding GF when the source point spans a basis cell $S_j$. And the averaged discrete GF is the "basis and test integrated GF," given by the mean value of the corresponding discrete GF when averaged over a test cell. With this notation, the elements of the MOM–Galerkin linear system (5) can be simply written as

$$c_{ij} = \Psi(S_i, S_j); \quad e_i = 4\pi\varepsilon_0 \frac{1}{S_i}\int_{S_i} ds\,[U - V_{\mathrm{exc}}(\mathbf{r})]. \tag{8}$$

The averaged discrete GFs, given by double surface integrals, can be approximated at different levels of accuracy. First, we can use the mean value theorem of integral calculus to evaluate the testing integrals (on the observer's $\mathbf{r}$ coordinates). This amounts to replacing the averaged discrete GF by a discrete GF computed at the center of the test cell; then, (8) can be approximated as

$$c_{ij} \simeq \Gamma(\mathbf{r}_i, S_j); \quad e_i \simeq 4\pi\varepsilon_0[U - V_{\mathrm{exc}}(\mathbf{r}_i)]. \tag{9}$$

The same result (9) could have been formally obtained by using Dirac's delta functions as test functions. This was the approach taken by Harrington, resulting in the MOM implementation, which he called "point matching" [1, Sec. 1.4]. The name is fully justified, because the PM approach boils down to satisfying the PIE (2) only at a set of discrete points (the cells' centers), where the potential created by the basis functions must be calculated.

In a further simplification, the mean value theorem is applied again, this time to the source integral. The result reduces the MOM matrix elements to simply the value of the GF evaluated at the center of the test and basis cells. This will be called the "GF approximation":

$$c_{ij} \simeq G(\mathbf{r}_i\,|\,\mathbf{r}_j). \tag{10}$$

Because of the singularity of our GF, this bold simplification cannot obviously be applied to the diagonal terms $c_{ii}$, but it will provide a first-order approximation if $i \neq j$.

In practice, approximations of different levels can be mixed when filling the MOM matrix, trying to achieve the best tradeoff among simplicity of the analytical developments, computer time, and accuracy of the results. After all, as noted above, all the possible combinations can be considered numerical approximations of the original Galerkin formulation [10].

For instance, a reasonable Galerkin implementation can use the rigorous expressions (8) only for self-interactions and possibly for the interaction among adjacent cells while computing all the remaining matrix elements with the approximations (9) or (10). In his book, Harrington frequently used a PM formulation (9) but with a liberal use of the drastic approximation (10), which was applied everywhere but in the diagonal elements [1, eq. 2.32]. Now we see clearly the benefits of our choice (6) for the basis functions. The MOM elements in the different approaches (8)–(10) are always given by GF values, possibly averaged over the cells' surfaces. This provides an easy check of the implementations and allows a direct comparison among the different MOM versions.

In the following sections, we review and complete some of Harrington's developments for the canonical case of parallel rectangular plates in free space.

## ANALYTICAL RESULTS FOR PARALLEL RECTANGULAR CELLS IN FREE SPACE

In his electrostatic examples, Harrington always considered free-space situations, allowing him to use the free-space GF $G(\mathbf{r}|\mathbf{r}') = 1/|\mathbf{r} - \mathbf{r}'|$. And he always used a PM approach, approximating his surfaces by a set of square cells with constant surface charge ("subareas," as he called them), even in the case of a hollow conducting cylinder [1, Sec. 2.3]. While all these restrictions were fully justified, taking into account the limited computational resources of his time, nowadays it is customary to consider more sophisticated choices like, for instance, Galerkin strategies using linear basis functions defined on triangular cells. In our community, this has been mostly done in the frame of scattering and antenna problems, where a frequency-dependent GF is needed. Therefore, we delay the discussion of this subject until the second part of this article, which deals with electrodynamics problems.

Harrington never considered a real application of the Galerkin approach in his book [1]. This is likely due to the fact that the analytical calculation of the generic 4D integrals (5b) is a formidable task. As for a purely numerical evaluation, this was probably not feasible in the 1970s and remains today a time-consuming task. On the other hand, a full analytical solution can be obtained for rectangular cells in free space, at least for some specific situations that include parallel and orthogonal orientations, although the complexity of the final formulas can be discouraging. See [11] for pioneering work and [12] for a recent more comprehensive study.

In this article, we pursue a more modest goal, limiting ourselves to a Galerkin formulation using piecewise constant functions defined on rectangular grids placed on parallel planes and sharing a common orientation. This generalization of Harrington's procedures is enough to ascertain the accuracy he reached, and it allows the study of other interesting problems, such as stacked parallel plates of different sizes. We consider uniform meshes with identical cells, all of dimensions $a \times b$.

In general, the $j$th basis cell has its center at $(x_j, y_j, z_j)$, and the $i$th test cell center is at $(x_i, y_i, z_i)$. We can always make a coordinate translation to put the lower-left corner of the basis cell at the origin of the coordinates. Then, as depicted in Figure 2, the lower-left corner of the test cell is at $(x_c, y_c, z_c)$, with $x_c = |x_i - x_j|$, $y_c = |y_i - y_j|$, and $z_c = |z_i - z_j|$. Notice that due to the symmetry of the GFs, we can assume that $x_c$ and $y_c$ are always positive. As for the third coordinate, we simply write $z_c = |z_i - z_j| = h$. With this notation, we make it clear that, since we consider only plates parallel to the $xy$-plane, the $z$-coordinates are never variables of integration but take a constant value $h$, which is simply the vertical distance between the plates (obviously, $h = 0$ if the $i$th and $j$th cells belong to the same plate).

Then, for plates embedded in free space, the MOM matrix elements $c_{ij}$ in (8) are given by

$$c_{ij} = \Psi(S_i, S_j) = \frac{1}{(ab)^2} \int_{x_c}^{x_c+a} dx \int_{y_c}^{y_c+b} dy$$
$$\times \int_0^a dx' \int_0^b dy' \frac{1}{\sqrt{(x-x')^2 + (y-y')^2 + h^2}}. \tag{11}$$

There is an enlightening mathematical interpretation of this equation. In free space, the static GF is just the inverse of the source–observer distance. Therefore, the quantity $1/\Psi$ (the inverse of our average discrete GF) can be viewed as the harmonic mean distance between two cells. And, correspondingly, $1/\Gamma$ is the harmonic mean distance between one cell and one point. So, Galerkin interactions between cells are equivalent to interactions between point charges separated by the harmonic mean distance between cells. Amazingly, this concept was familiar to Maxwell himself, who used it in a paper published in 1872 and entitled "On the Geometrical Mean Distance of Two Figures on a Plane" [13].

The 4D integral can be easily solved analytically through the use of a smart change of variables, which reduces the 4D integral in (11) to a 2D integral in the new variables $u = x - x'$ and $v = y - y'$ and leads to full analytical expressions for the MOM matrix elements, as explored further in the supplementary
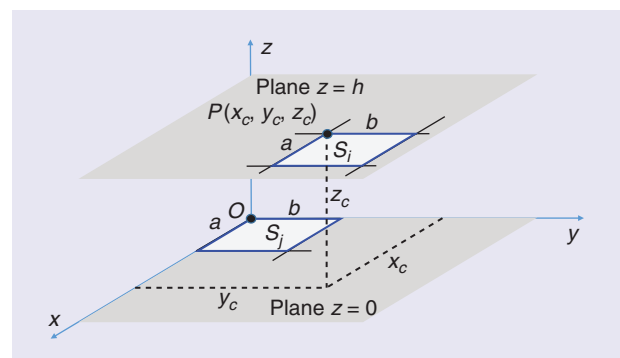


**FIGURE 2.** Basis and test cells of equal size and orientations and located in parallel planes. A corner of the basis cell is centered at the origin of the coordinates. The coordinates of the test cell's corresponding corner are ($x_c$, $y_c$, $z_c$).

material available at https://doi.org/10.1109/MAP.2024.3362249. The reduced 2D integral is

$$c_{ij} = \frac{1}{(ab)^2} \int_{y-b}^{y+b} dv \int_{x-a}^{x+a} du \, \frac{\Lambda(u)\,\Lambda(v)}{\sqrt{u^2 + v^2 + h^2}} \qquad (12)$$

where the triangular functions $\Lambda$ are defined as

$$\Lambda(u) = \begin{cases} u - x_c + a \;; & x_c - a < u < x_c \\ x_c + a - u \;; & x_c < u < x_c + a \end{cases};$$
$$\Lambda(v) = \begin{cases} v - y_c + b \;; & y_c - b < v < y_c \\ y_c + b - v \;; & y_c < v < y_c + b \end{cases}. \qquad (13)$$

These triangular functions can be viewed as the cross correlation or convolution of two pulse functions [14, Secs. 12-2 and 12-3]. In general, this change of variables transforms a 4D integral involving a basis function and a test function into a 2D integral involving the correlation of these basis and test functions, as expounded in the supplementary material. Similar devices have been previously used by other researchers. See, for instance, [15].

Inside the double integral (12), there are four different integrals because the product of the triangular functions (13) will always result in a polynomial $Auv + Bu + Cv + D$. The evaluation of (12) is then made by finding the 2D primitives (indefinite double integrals) and invoking a generalized fundamental theorem of calculus (see the supplementary material).

The calculation of the 2D primitives of these four integrals can be attempted using symbolic integration tools (Maple, Mathematica, MATLAB, the open source Python SymPy, and so on). But the results are sometimes disappointing and frequently hard to compare with classical results. Anyway, it would be a pity to renounce the pleasures of doing calculations by hand (a vanishing precomputer wisdom). The four primitives needed are given in Table 1, and additional details are available in the supplementary material.

These analytical formulas allow a complete analytical evaluation of our MOM matrix elements in (11). The first row in Table 1 is a generalization a well-known expression, given by Wintle [16] for purely coplanar situations ($h = 0$):

$$\int du \int dv \frac{1}{\sqrt{u^2 + v^2}} = u \sinh^{-1}(v/|u|) + v \sinh^{-1}(u/|v|). \qquad (14)$$

This is a very simple 2D primitive, yet it is hard to obtain it with symbolic software tools (see the supplementary material).

With the use of these primitives, all the Galerkin MOM matrix elements can be analytically computed. This allows us to solve practical problems involving single or parallel rectangular plates in the Galerkin framework. As a straightforward application, let us find the effect of a rectangular cell on itself (the diagonal terms in a Galerkin formulation). Here, we have $h = 0$ and $x_c = y_c = 0$. Then, by symmetry, (12) reduces to

$$c_{ij} = \frac{4}{(ab)^2} \int_0^b dv \int_0^a du \, \frac{(u-a)(v-b)}{\sqrt{u^2 + v^2}}$$
$$= \frac{2}{b} \sinh^{-1} \frac{b}{a} + \frac{2}{a} \sinh^{-1} \frac{a}{b} + \frac{2}{3a^2 b^2}[(a^3 + b^3) - (a^2 + b^2)^{3/2}]. \qquad (15)$$

This interesting result has been obtained by a direct application of (13) combined with the primitives of Table 1. But for this particular case, the integral (15) is much easier and can be directly evaluated using polar coordinates. This provides a useful check of our work.

For the particular case of a unit square cell ($a = b = 1$), we have the result

$$c_{ii} = \int_0^1 dx \int_0^1 dy \int_0^1 dx' \int_0^1 dy' \frac{1}{\sqrt{(x-x')^2 + (y-y')^2}}$$
$$= 4 \sinh^{-1}(1) - \frac{4}{3}(\sqrt{2} - 1) = 2.9732. \qquad (16)$$

## TABLE 1. THE 2D PRIMITIVES NEEDED FOR (12).

| Function | Primitive |
|---|---|
| $f(u, v)$ | $F(u, v) = \iint du\,dv\,f(u, v)$ |
| $\dfrac{1}{\sqrt{u^2 + v^2 + h^2}}$ | $u \sinh^{-1}\left(\dfrac{v}{\sqrt{u^2 + h^2}}\right) + v \sinh^{-1}\left(\dfrac{u}{\sqrt{v^2 + h^2}}\right) - h \tan^{-1}\left(\dfrac{uv}{h\sqrt{u^2 + v^2 + h^2}}\right)$ |
| $\dfrac{u}{\sqrt{u^2 + v^2 + h^2}}$ | $\dfrac{1}{2}\left[v\sqrt{u^2 + v^2 + h^2} + (u^2 + h^2)\sinh^{-1}\left(\dfrac{v}{\sqrt{u^2 + h^2}}\right)\right]$ |
| $\dfrac{v}{\sqrt{u^2 + v^2 + h^2}}$ | $\dfrac{1}{2}\left[u\sqrt{u^2 + v^2 + h^2} + (v^2 + h^2)\sinh^{-1}\left(\dfrac{u}{\sqrt{v^2 + h^2}}\right)\right]$ |
| $\dfrac{uv}{\sqrt{u^2 + v^2 + h^2}}$ | $\dfrac{1}{3}(u^2 + v^2 + h^2)^{3/2}$ |

Care must be exerted when evaluating some of these primitives in the particular case when $h = 0$ and the variables $u$ or $v$ vanish. In practical implementations, a not very rigorous (but really practical) trick is always to avoid the coplanar situation by replacing the theoretical zero value of $h$ for the smallest nonzero value accepted by the computer language being used. Fortunately enough, this situation arises only when potentials are computed in the edges of the cells, which is not a usual need in MOM calculations.

This nice result has an interesting physical interpretation. In the self-case, Harrington's strategy of replacing cells by point charges located in the cells' centers cannot be applied. But in a Galerkin strategy, the interaction between cells is equivalent to the interaction between point charges separated by the harmonic mean distance between cells. For the interaction of a unit square cell with itself (the MOM diagonal self-case), this distance is not zero. Rather, according to (16), it has a value $1/2.9732 = 0.3363$, practically one-third of the cell's side.

If, instead of Galerkin, a PM strategy is used, we apply the mean value theorem to (11), with the result

$$c_{ij} = \Gamma(\mathbf{r_i}, S_j) = \frac{1}{ab} \int_0^b dy' \int_0^a dx'$$
$$\times \frac{1}{\sqrt{(x_c + a/2 - x')^2 + (y_c + b/2 - y')^2 + h^2}}. \quad (17)$$

Again, the first row of Table 1 provides the complete solution of this integral. In this case, it could be more practical to define the origin of coordinates at the center of the source cell. Then, it becomes obvious that the above expression gives the normalized potential created at a point $(x_c, y_c, h)$ by a rectangular cell of dimensions $a \times b$ located in the $xy$-plane, centered at the origin and with unit total charge. For the particular case of a square cell $(a = b)$ with unit total charge and points in its normal axis $(x_c = y_c = 0)$, we find the interesting result

$$4\pi\varepsilon_0 V_{\text{axis}}(0,0,h) = \frac{4}{a} \sinh^{-1}\left(\frac{a}{\sqrt{a^2 + 4h^2}}\right)$$
$$- \frac{4h}{a^2} \tan^{-1}\left(\frac{a^2}{2h\sqrt{2a^2 + 4h^2}}\right). \quad (18a)$$

Another special case of (17) is the PM self-case, with $x_c = y_c = 0$ and $h = 0$, which corresponds to the potential of a rectangular cell on its center:

$$c_{ii} = 4\pi\varepsilon_0 V_{\text{center}} = \frac{2}{a} \sinh^{-1}(a/b) + \frac{2}{b} \sinh^{-1}(b/a) \quad (18b)$$

an expression which, in the particular case $a = b$ (a square cell), fully agrees with the one given by Harrington [1, eq. 2.31] once the inverse hyperbolic sines are expressed as logarithms. In particular, for the unit square cell, we obtain the well-known numerical value $c_{ii} = 3.5255$.

## IMPLEMENTATION AND TEST OF THE ANALYTICAL EXPRESSIONS FOR DISCRETE AND AVERAGED DISCRETE GFs

The analytical expressions for the discrete GF $\Gamma_{ij}$ (17) and the averaged discrete GF $\Psi_{ij}$ (11) have been implemented as the MATLAB functions `DiscrGF` and `AvDiscrGF`, respectively (see the supplementary material). Basis and test cells have the same dimensions $a \times b$ and the same orientation. For the implementation, it has been found handy to center the basis cell at the origin of coordinates. Then, the test cell center is at $(x_c, y_c, z_c)$.

As a preliminary step, the analytical values of $\Gamma_{ij}$ and $\Psi_{ij}$ have been checked by making a rough direct numerical

integration of the two-fold integral in (17) and the four-fold integral in (11) using standard quadratures. The results of these quadratures always converge toward the analytical values, although the convergence can be very slow and require a very large number of evaluation points if the basis and test cells are partially or totally overlapping. This is an additional proof for the validity of the analytical expressions, which are not only practically unavoidable for the self-case but can also save significant amounts of computer time in Galerkin approaches when cells are adjacent or close.

Once the analytical expressions of discrete and averaged discrete GFs have been checked numerically, it is interesting to compare their values to foresee the possible differences that could be observed if different MOM approaches were applied to the same problem. For the comparison, we consider unit square cells $(a = b = 1)$.

Figure 3(a) provides, for a coplanar case with both cells in the $(z = 0)$-plane, a graphical comparison among the three
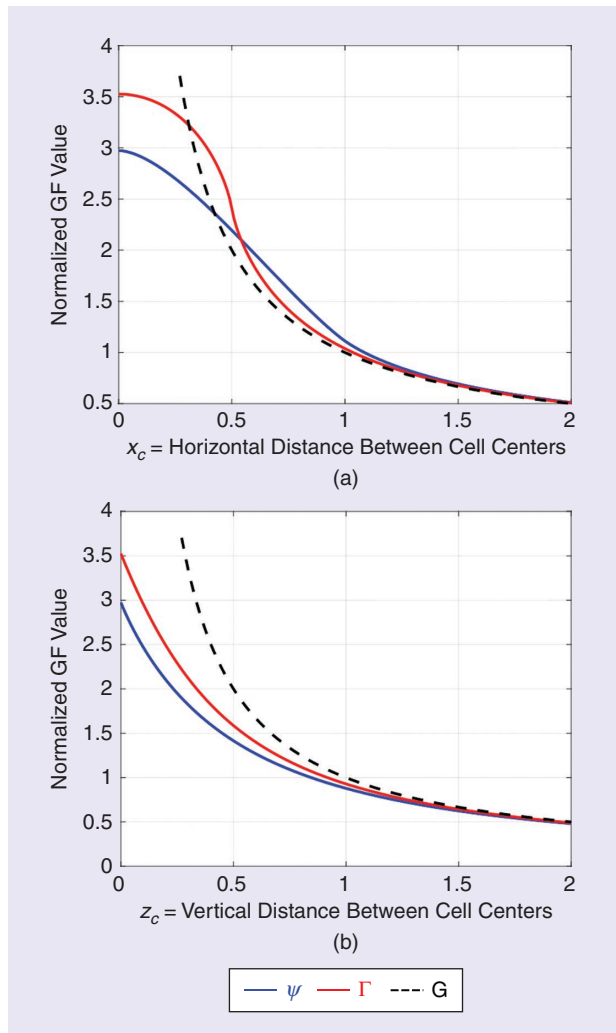


**FIGURE 3.** Results for averaged discrete values (Galerkin, $\Psi$), discrete values (PM, $\Gamma$), and plain values ($G$) of the static free-space GF. (a) The cells are centered on the $x$-axis (coplanar cells). (b) The cells are centered on the $z$-axis (parallel cells). Unit square cells are considered.

possible strategies, using $\Psi$, $\Gamma$, and the plain GF approximation $G$. Here, the basis cell is centered at the origin, and the test cell has its center on the $x$-axis at $(x_c, 0, 0)$, with $0 < x_c < 2$. The functions $\Psi, \Gamma$, and $G$ (given here simply by $G = 1/x_c$) are depicted, respectively, with blue, red, and dashed black lines. While not evident in the plot, finer calculations with the same script show that the red line has an infinite derivative at $x_c = 0.5$, which corresponds to the physical fact that the electric field is infinite at the edges of a charged plate. For distances roughly smaller than the cell half-size, $\Gamma$ (PM) is greater than $\Psi$ (Galerkin), but for larger distances, the $\Gamma$ values remain systematically below $\Psi$. Then, in Figure 3(b), we explore, with the same color codes, the situation where the center of the test cell is located along the $z$-axis at $(0, 0, z_c)$, with $0 < z_c < 2$. Here, $\Gamma$ is always larger than $\Psi$ and closer to GF values ($G = 1/z_c$). The discrepancies in the self-case ($x_c = z_c = 0$) are quite significant, with $\Psi$ being 18.6% smaller than $\Gamma$. But, for adjacent coplanar cells, $\Psi$ is slightly larger than $\Gamma$ (6.6%). As expected, the Galerkin dynamic range for the MOM matrix is lower than the PM range since it involves an extra averaging over the test cell.

The Green's approximation (not valid in the self-case) produces a large error in adjacent cells calculations (4% and 11% with respect to $\Gamma$ and $\Psi$). But, as expected, both $\Gamma$ and $\Psi$ values converge quickly toward plain GF values, the differences between the three approaches being less than 0.5% when the distances between cells are larger than five times the cells' sides.

Therefore, it seems quite reasonable to replace $\Psi$ or $\Gamma$ values by approximated GFs when computing interactions between cells separated by a distance above a given threshold (say, three or four times a cell's size). On the other hand, the bold Harrington strategy, replacing all PM values outside the main diagonal by GF values, seems a priori quite risky.

In any case, it is not mathematically easy to predict how a change in some elements of a linear system matrix will affect the values of the linear system solution (in our case, electric charge densities and capacitances). So, let us solve the problem and observe the results a posteriori.
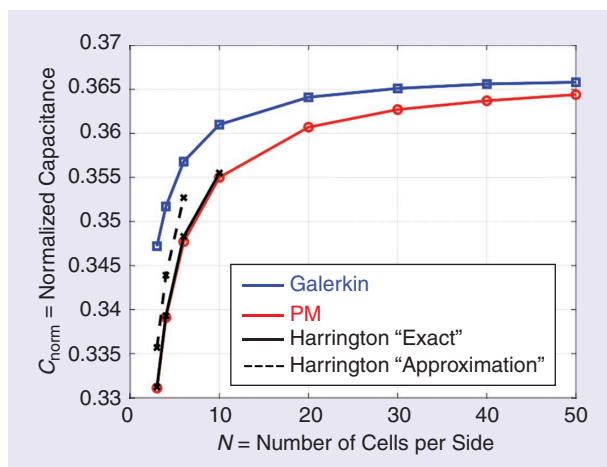


**FIGURE 4.** Normalized square plate capacitances for different MOM strategies as a function of the number $N$ of cells per side (the total number of cells in the plate is $N^2$).

## SINGLE PLATE AT CONSTANT POTENTIAL

We consider now the first electrostatic problem discussed by Harrington [1, Sec. 2.2], the classic problem of a square unit metallic plate at a constant potential. Both the Galerkin and PM strategies have been implemented in a simple MATLAB script `StaticPlate` (see the supplementary material), which is able to deal with parallel rectangular plates divided into rectangular cells and optionally permits Harrington's simplification of using plain GF values as matrix elements. Because the analytical values of $\Gamma_{ij}$ and $\Psi_{ij}$ are used, no numerical integration routines are needed, and the construction of the MOM matrix is simple and straightforward. For the excitation vector, several classical options have been considered, and the linear system is simply solved with the standard MATLAB backslash "\" command. The solution vector contains the values of the total charges in every cell.

We consider first a single plate of dimensions $A \times B$ m divided into $M \times N$ rectangular cells and at a fixed potential $4\pi\varepsilon_0 U = 1$. To reproduce Harrington's square plate, we select $A = B$ and $M = N$. Then, the total charge on the plate, which is the sum of all the cells' charges, gives directly the normalized capacitance $C_{\text{norm}}$. For a square plate of side $A$, the true capacitance in farads is $C = 4\pi\varepsilon_0 A C_{\text{norm}}$. Using the PM option, the MATLAB script `StaticPlate` allow us to recover the charge values and the square plate capacitances given by Harrington in his book. But, of course, we can now also try a Galerkin formulation and higher numbers of cells.

Figure 4 provides the results obtained for the normalized capacitance $C_{\text{norm}}$ of a unit square plate ($A = 1$) versus the number of cells $N$ existing in the side of the plate, using both PM and Galerkin approaches. The two curves in black with crosses reproduce Harrington's results using his two PM strategies [1, Table 2.1]. Serendipity was at work here because the "rough approximation" scheme of Harrington (the dashed black line) gave better results than his "exact" values (the black continuous line).

For this problem, Harrington stopped his calculations with only 36 unknowns ($N = 6$). We have reproduced his results and extended his curve up to 2,500 unknowns ($N = 50$) in the red curve with circles, where we can observe the typical slow convergence of PM. In the same figure, we have plotted the results obtained with a simplified Galerkin strategy (the blue curve with squares). The results are better and exhibit a faster convergence. A Galerkin result with 400 unknowns is already much more accurate than a PM with 2,500 unknowns. So, at least in some situations, it seems better to go for Galerkin and use a smaller number of unknowns despite the increased analytical complexity.

Harrington's results were already good enough from an engineering point of view, his best point showing only a 3% error with respect to a converged Galerkin. And Harrington was able to extrapolate his results, asserting that "a good estimate of the true capacitance is 40 picofarads" [1, Sec. 2.2]. This corresponds to $C_{\text{norm}} = 0.36$, while our best Galerkin extrapolation is $C_{\text{norm}} = 0.3671$ ($C = 40.79$ pF/m), practically identical to the "best existing result," $C_{\text{norm}} = 0.367$ (40.78 pF/m), published by Noble in 1971 [18], as duly acknowledged by Wintle [16] and

reviewed by Kuester in his comprehensive survey paper [19] on microstrip patch capacitances.

Interestingly enough, in 1879, Maxwell himself had anticipated Harrington's strategy, using what we would call now a PM approach, when trying to provide a numerical justification to the empirical results of Cavendish for the capacitance of a square plate [20]. Maxwell cut the plate into $6 \times 6$ cells; hence, the number of MOM unknowns would have been 36, but a clever use of symmetry reduced the total to only six different unknowns. In an orthodox MOM approach, all the values of the diagonal elements $c_{ii}$ must be identical if all the cells are identical. However, Maxwell's approach was rather unorthodox because he slightly tweaked the results for the diagonal elements and made them dependent on the cell position (center, edge, and corner) within the square plate. In addition, it seems that Maxwell made some numerical errors when solving his linear system of six unknowns by hand. Nevertheless, Maxwell was able to announce a value $C_{norm} = 0.361$ ($C = 40.1$ pF/m), within Cavendish experimental values ($C = 40 - 41.6$ pF/m) and perfectly aligned with modern results. This fascinating story has been studied in great detail by Wintle [16], who concluded his paper with a somewhat irreverent but justified remark: "Evidently, Maxwell was not at the top of his form on this occasion."

## PARALLEL PLATE CONDENSER

As a second example, we consider the parallel plate condenser formed by two parallel square plates of side $A$ separated by a distance $h$. This is a classic example treated by Harrington [1, Sec. 2.4] that became very relevant a few years later, when microstrip technology boomed in the early 1970s [21]. Harrington did not make any use of symmetry between the two plates (this would be the correct approach when the plates are different). However, in a standard configuration, the plates are identical, and we can always assume they are at potentials $\pm V$ and exhibit identical charges, albeit of opposite sign $\pm Q$. Then, it is still possible to use our script `StaticPlate`, modifying the GF as $G(\mathbf{r}|\mathbf{r}') = 1/|\mathbf{r} - \mathbf{r}'| - 1/|\mathbf{r} - \mathbf{r}' + h\hat{\mathbf{e}}_{\mathbf{z}}|$ and applying the MOM to just one plate. Once the total charge $Q$ in the plate has been calculated, the capacitance is simply given by $C = |Q|/2V$. Following Harrington, we concentrate on the calculation of the "fringing factor" $C/C_0$, where $C$ is the MOM capacitance (thus including fringing fields) and $C_0$ is the classic parallel plate conductor formula, obtained by neglecting the fringing fields: $C_0 = \varepsilon_0 A^2/h$.

Figure 5 gives the values of the fringing factor $C/C_0$ as a function of the normalized distance between plates $h/A$. Several approaches have been considered. The continuous blue curve gives the results obtained with a converged MOM implementation ($N > 10$ in Galerkin, and $N > 20$ in PM), while the black curve reproduces as accurately as possible the results given by Harrington [1, Fig. 2.7] for a shorter range of the distances between plates $0.1 < h/A < 1.0$ (see the supplementary material).

The differences between these curves can be attributed to the insufficient discretization of the plate used and/or to some approximations used by Harrington [1, eq. 2.43]. Indeed, if the PM version of our code is run with a lower number of cells

($N = 6$), we obtain the dashed red curve, which is practically on top of Harrington's results and also agrees with Farrar and Adams [21]. Finally, the dotted blue curves correspond to the analytical asymptotic approximations for "small and large patches," given by Kuester in his complete study of microstrip patch capacitances [18, eqs. 2.15 and 3.36]. Our numerical MOM results are perfectly framed by Kuester's asymptotic expressions.

A word of warning is needed because Harrington's results [1, Fig. 2.7] are slightly different in the three editions of his book (see the supplementary material). Here, we have used the values extracted from the last (1993) edition, which seem the best or, at least, the ones closest to our PM results and to the numerical results obtained in 1972 by Farrar and Adams in their classic study of microstrip patches capacitances [21].

## SINGLE PLATE EXCITED BY A POINT CHARGE

With minor modifications, the script `StaticPlate` can be used for many other interesting problems, for instance, to study the shielding effect of a metallic plate on the electric field created by a nearby point unit charge $q$ placed at $\mathbf{r}_q$. In this case, the excitation vector components (9) are given by $e_i = -q/|\mathbf{r}_i - \mathbf{r}_q|$. We have selected a unit square plate in the $z = 0$-plane, with vertexes at (0,0,0), (1,0,0), (0,1,0), and (1,1,0). A unit positive point charge is located above the plate center at (0.5,0.5,0.5). Our MATLAB script using $20 \times 20$ cells and a PM strategy predicts a total induced charge in the plate $Q = -0.538$, which shows clearly that not all the field lines starting from the point charge are ending in the plate. The value obtained with Galerkin is less than 1% different. To check the validity of our calculations, we have plotted in one midplane of the plate $y = 0.5$ the total potential due to the unit point charge and to the negative surface charge induced in the plate:

$$4\pi\varepsilon_0 V(\mathbf{r}) = \frac{q}{|\mathbf{r} - \mathbf{r_q}|} - \int_S ds' \frac{\rho_s(\mathbf{r}')}{|\mathbf{r} - \mathbf{r}'|}$$

$$\approx \frac{q}{|\mathbf{r} - \mathbf{r_q}|} - \sum_{i=1,N} \frac{\alpha_i}{|\mathbf{r}_i - \mathbf{r_q}|} \quad (19)$$
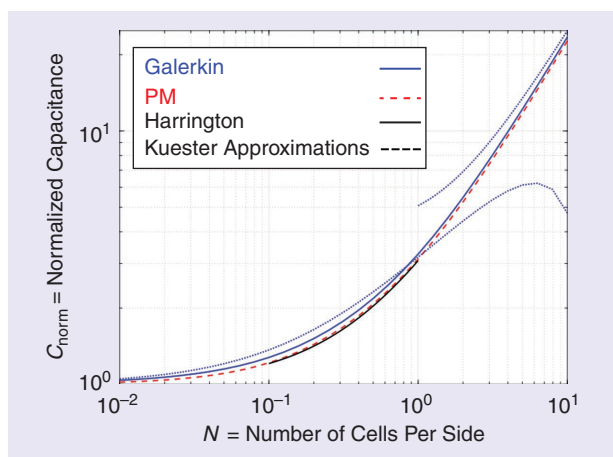


**FIGURE 5.** The fringing factor $C/C_0$ of a square parallel plate capacitor as a function of the normalized distance between plates $h/A$.

where the summation is to be extended to all the cells in the plate.

Figure 6 displays the results obtained after adding the above equation to our MATLAB script `StaticPlate` and using the command `contourf` to visualize the equipotential lines. The deformation produced by the plate on these lines corresponds to the physics of the problem. Some lines still enclose
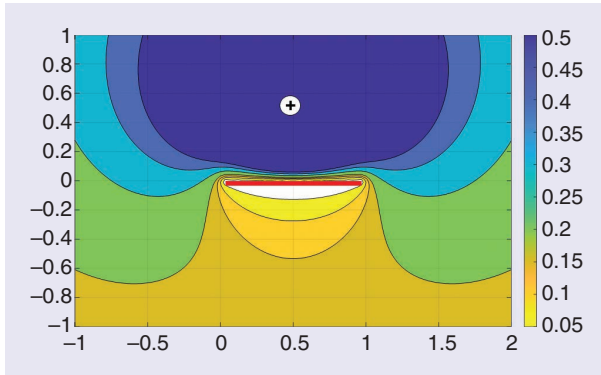
the point charge while trying to go around the plate. Other lines do not enclose the point charge any longer but do enclose the plate, and the equipotential zero becomes the plate itself. Also, the concentration of the lines just above the plate tells us about strong field values there.

## 3D PLOTS

In the 1960s, 3D plots were only a researcher's dream; no wonder that they cannot be found in Harrington's book. Today, however, they are routinely offered by popular software tools like MATLAB.

Figure 7 contains several 3D plots of the normalized surface charge density, obviously obtained by dividing the total charge in every cell (the unknowns in our MOM implementation `StaticPlate`) by the cell's surface areas. A relatively modest grid of $20 \times 20$ cells has been used.

Figure 7(a) and (b) refers to the single plate of the "Single Plate at Constant Potential" section. Two drawing strategies have been used. In Figure 7(a), the values of the piecewise constant basis functions in every cell have been depicted as realistically as possible. In Figure 7(b), we have just plotted the same numerical values using the MATLAB command `surf`.
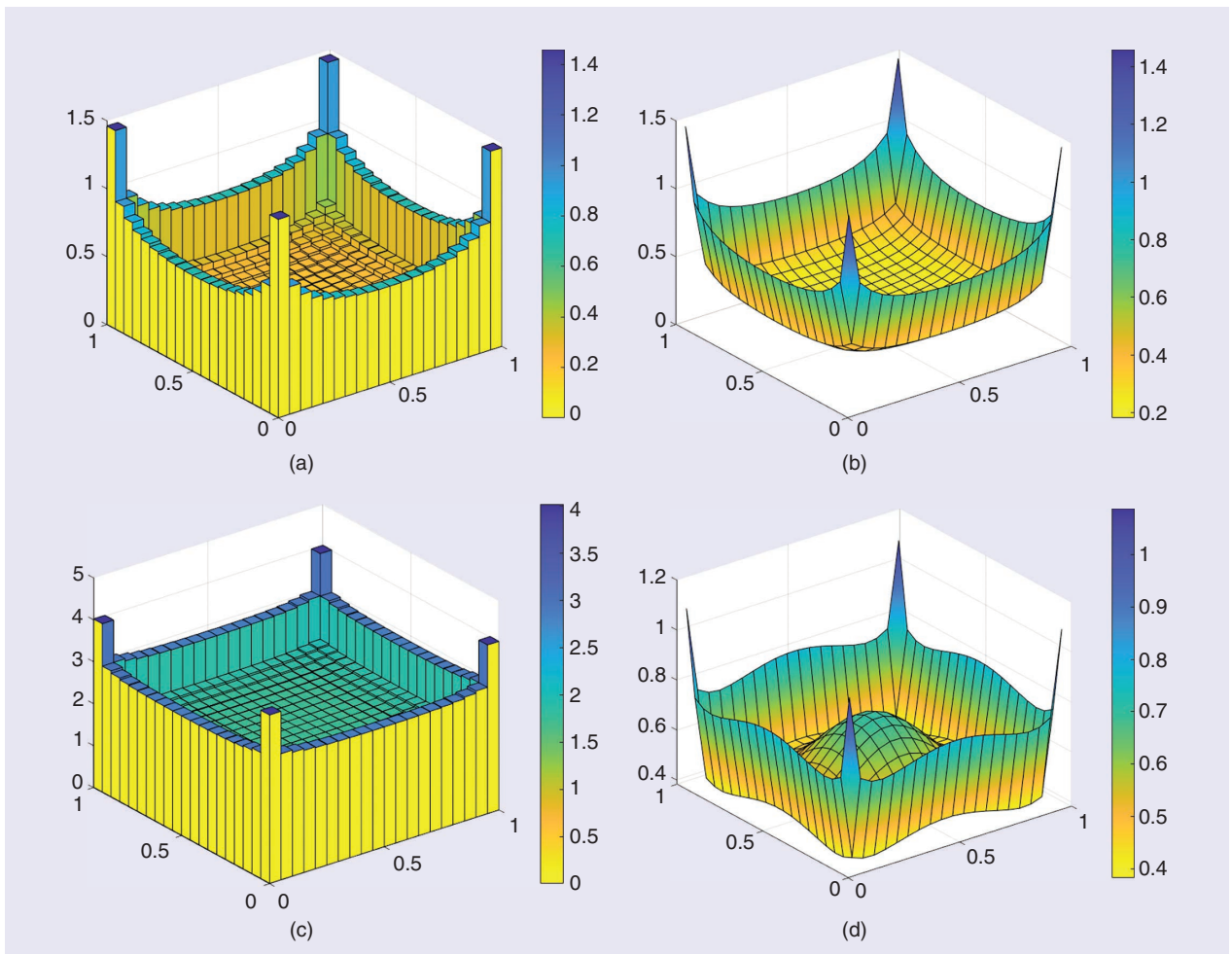
**FIGURE 6.** Equipotential lines in the median plane of a square plate excited by a point charge above its center.

**FIGURE 7.** The surface charge distribution in (a) and (b) an isolated plate; (c) the upper plate of a parallel plate condenser, with $h/A = 0.1$; and (d) a plate excited by a point charge above it and on its normal axis.

Observing these two graphs, one wonders whether the interpolation scheme in the plotting routine `surf` is producing a result equivalent to the one we could have obtained using higher-order basis functions, such as piecewise linear ones.

In Figure 7(c), the charge density is that existing in the upper plate of a parallel plate condenser with $A = 1$ and $h/A = 0.1$ (the "Parallel Plate Condenser" section). It is interesting to compare the graph with that in Figure 7(a) corresponding to a single plate ($h \to \infty$). Of course, here, a quantitative comparison is meaningless. But the change in the shape of the charge density is remarkable, the two close plates of a parallel condenser resulting in a much more uniform distribution, save for the well-known edge fringing effects. Finally, Figure 7(d) is a `surf` plot of the absolute value of the negative charge density appearing in the problem of the "Single Plate Excited by a Point Charge" section. The effect of the point charge is clearly apparent as a "bulge" in the center of the plate and a slight distortion of the charge profile in the edges of the plate.

All the results used to generate Figure 7 were obtained using a PM approach. But no differences visible to the naked eye would appear if a Galerkin strategy were used. A closer comparison, using $50 \times 50$ cells and singling out the values of the charge in the median line of the plate (as done in [1, Fig. 2.2]), reveals that the differences between the surface charge density values obtained by using PM and Galerkin strategies remain below 1% except for the cells closer to the edges, where differences of up to 7% can be observed. These differences near edges and corners are not surprising at all. Charge distributions with singularities cannot be exactly simulated with bounded basis functions. Fortunately enough, the integration (here, the sum) of the cells' charge values is an error canceling process, and simple pulse basis functions are enough to obtain remarkably accurate results for the capacitance values.

While we should always expect Galerkin to perform better than PM when approaching a regular continuous function, this is not granted in problems involving singular surface charge distributions. Of course, it is always possible to select higher-order basis functions, possibly including singular behaviors. This is still an ongoing hot topic, as can be seen in recent works [22], [23]. Systematic convergence studies and detailed comparisons of different possible basis/test function choices are outside the scope of this article and have been treated in several authoritative books [5], [24], [25].

## CONCLUDING REMARKS

In this first part of the article, we concentrated on revisiting some electrostatics examples included by Harrington in his epoch-making book *Field Computation by Moment Methods*. While checking his pioneering results and highlighting their excellent quality, we have generalized them into a fully analytical formulation, which provides a systematic treatment and illuminating insights for configurations not previously treated. Our study has also allowed us to unearth some interesting historical facts that are barely known nowadays. It might be considered superfluous to treat in such a detail a series of purely electrostatic situations, especially in an antennas and propagation publication.

But this would be shortsighted. As discovered by Harrington himself, when time-harmonic full-wave problems are formulated in the context of a mixed PIE (MPIE), the mathematical parallelisms with the static PIE make all the electrostatic formulations developed here not only useful but also unavoidable when dealing with electrodynamic problems. Indeed, a reasonably accurate free-space MPIE software tool can be built by using the static discrete GFs developed here. In fact, the only additional complexity is that we will be dealing with a vectorial unknown (the electrodynamic surface current density) rather than with a scalar one (the electrostatic surface charge density). This will be clearly demonstrated in the second part of this article.

## ACKNOWLEDGMENT

## AUTHOR INFORMATION

**Juan R. Mosig** (juan.mosig@epfl.ch) is with École Polytechnique Fédérale de Lausanne, CH-1015 Lausanne, Switzerland. He is a Life Fellow of IEEE.

## REFERENCES

[1] R. F. Harrington, *Field Computation by Moment Methods* (1st ed. New York, NY, USA: Macmillan, 1968; 2nd ed. Malabar, FL, USA: Krieger, 1982), 3rd ed. Piscataway, NJ, USA: IEEE Press (Series on Electromagnetic Wave Theory), 1993.
[2] R. F. Harrington, "Origin and development of the method of moments for field computation," *IEEE Antennas Propag. Mag.*, vol. 32, no. 3, pp. 31–35, Jun. 1990, doi: 10.1109/74.80522.
[3] L. Kantorovich and G. Akilov, *Functional Analysis in Normed Spaces*, (Transl.: in D. E. Brown, Ed., Oxford: Pergamon, 1964, pp. 586–587).
[4] E. K. Miller, L. Medgyesi-Mitschang, and E. H. Newman, Eds., *Computational Electromagnetics: Frequency-Domain MoM*. Piscataway, NJ, USA: IEEE Press, 1992.
[5] W. C. Gibson, *The Method of Moments in Electromagnetics*, 3rd ed. London, U.K.: Chapman & Hall, 2021.
[6] R. F. Harrington, *Time-Harmonic Electromagnetic Fields* (Reissued from 1961). Piscataway, NJ, USA: IEEE Press (Series on Electromagnetic Wave Theory) 2001.
[7] D. R. Wilton, "History of developments leading to the method of moments," in *Proc. Int. Appl. Comput. Electromagn. Soc. Symp. (ACES)*, 2018, pp. 1–2, doi: 10.23919/ROPACES.2018.8364227.
[8] R. F. Harrington, "Matrix methods for field problems," *Proc. IEEE*, vol. 55, no. 2, pp. 136–149, Feb. 1967, doi: 10.1109/PROC.1967.5433.
[9] J. C. Rautio, "Roger Harrington and shielded planar microwave electromagnetic analysis," in *Proc. Int. Appl. Comput. Electromagn. Soc. Symp. (ACES)*, 2018, pp. 1–2, doi: 10.23919/ROPACES.2018.8364225.
[10] A. R. Djordjević and T. K. Sarkar, "A theorem on the moment methods," *IEEE Trans. Antennas Propag.*, vol. 35, no. 3, pp. 353–355, Mar. 1987, doi: 10.1109/TAP.1987.1144097.
[11] S. Lopez-Pena and J. R. Mosig, "Analytical evaluation of the quadruple static potential integrals on rectangular domains to solve 3-D electromagnetic problems," *IEEE Trans. Magn.*, vol. 45, no. 3, pp. 1320–1323, Mar. 2009, doi: 10.1109/TMAG.2009.2012613.
[12] M. De Lauretis et al., "On the rectangular mesh and the decomposition of a Green's-function-based quadruple integral into elementary integrals," *Eng. Anal. Boundary Elements*, vol. 134, pp. 419–434, Jan. 2022, doi: 10.1016/j.enganabound.2021.09.029.
[13] J. C. Maxwell, "XXIII— On the geometrical mean distance of two figures on a plane," *Trans. Roy. Soc. Edinburgh*, vol. 26, no. 4, pp. 729–733, 1872, doi: 10.1017/S008045680002559X.

[14] A. Papoulis, *The Fourier Integral and Its Applications*. New York, NY, USA: McGraw-Hill, 1962.

[15] T. F. Eibert and V. Hansen, "On the calculation of potential integrals for linear source distributions on triangular domains," *IEEE Trans. Antennas Propag.*, vol. 43, no. 12, pp. 1499–1502, Dec. 1995, doi: 10.1109/8.475946.

[16] H. J. Wintle, "Maxwell and the boundary element method: A historical puzzle," *IEEE Elect. Insul. Mag.*, vol. 14, no. 6, pp. 23–25, Nov./Dec. 1998, doi: 10.1109/57.730805.

[17] J. H. Wilkinson, *Rounding Errors in Algebraic Processes* (Prentice-Hall Series in Automatic Computation). Englewood Cliffs, NJ, USA: Prentice-Hall, 1963.

[18] B. Noble, "Some applications of the numerical solution of integral equations to boundary value problems," in *Proc. Conf. Appl. Numerical Anal.*, J. L. L. Morris, Ed., Berlin, Germany: Springer-Verlag, 1971, pp. 137–154.

[19] E. F. Kuester, "Explicit approximations for the static capacitance of a microstrip patch of arbitrary shape," *J. Electromagn. Waves Appl.*, vol. 2, no. 1, pp. 103–135, 1988, doi: 10.1163/156939387X00289.

[20] J. Clerk Maxwell, Ed., *Electrical Researches of the Honourable Henry Cavendish*, Cambridge, U.K.: Cambridge Univ. Press, 1879, pp. 426–427. [Online]. Available: https://archive.org/details/electricalresear00caveuoft/page/426

[21] A. Farrar and A. T. Adams, "Matrix methods for microstrip three-dimensional problems," *IEEE Trans. Microw. Theory Techn.*, vol. 20, no. 8, pp. 497–504, Aug. 1972, doi:[ 10.1109/TMTT.1972.1127796.

[22] A. F. Peterson and R. D. Graglia, "Relative impact of singular edge and corner basis functions on the capacitance of parallel-plate capacitors," in *Proc. Int. Conf. Electromagn. Adv. Appl. (ICEAA)*, Honolulu, HI, USA, 2021, pp. 414–415, doi: 10.1109/ICEAA52647.2021.9539526.

[23] R. D. Graglia, A. F. Peterson, and P. Petrini, "Hierarchical divergence conforming bases for tip singularities in quadrilateral cells," *IEEE Trans. Antennas Propag.*, vol. 68, no. 12, pp. 7986–7994, Dec. 2020, doi: 10.1109/TAP.2020.3026900.

[24] R. Mittra and C. A. Klein, "Stability and convergence of moment method solutions," in *Numerical and Asymptotic Techniques in Electromagnetics*, R. Mittra, Ed., New York, NY, USA: Springer-Verlag, 1975, pp. 129–163.

[25] A. F. Peterson, S. L. Ray, and R. Mittra, *Computational Methods for Electromagnetics*. Hoboken, NJ, USA: Wiley-IEEE Press, 1997.